

CEBAF-PR-87-018 VWC3  
H.A. Gruner  
Superconducting Acc\Technology  
\* 020592000096220



R020592000096270B

CEBAF-PR-87-018

## SUPERCONDUCTING ACCELERATOR TECHNOLOGY

*Hermann A. Gruner and Beverly K. Hartline  
Continuous Electron Beam Accelerator Facility  
12070 Jefferson Avenue  
Newport News, VA 23606*

# SUPERCONDUCTING ACCELERATOR TECHNOLOGY

Hermann A. Grunder and Beverly K. Hartline  
Continuous Electron Beam Accelerator Facility  
Newport News, VA 23606

## ABSTRACT

Modern and future accelerators for high energy and nuclear physics rely increasingly on superconducting components to achieve the required magnetic fields and accelerating fields. This paper presents a practical overview of the phenomenon of superconductivity, and describes the design issues and solutions associated with superconducting magnets and superconducting rf accelerating structures. Further development and application of superconducting components promises increased accelerator performance at reduced electric power cost.

## INTRODUCTION

When H. Kamerlingh Onnes discovered the phenomenon of superconductivity 75 years ago<sup>1</sup> (Figure 1), he recognized that its exploitation could give rise to highly efficient electrical apparatus operating with no resistive losses, exotic new devices, and the production of intense magnetic fields. Although Onnes was frustrated in his attempts to produce high magnetic fields, because the field



Fig. 1. H. K. Onnes (seated) with J. van der Waals with the first helium liquifier.

itself drove his superconductors normal, the technological capabilities he envisioned have largely been achieved today.

For application to particle accelerators, superconducting technology has entered into an extremely rewarding phase. Its benefits are increased performance at reduced operating cost. Present and planned accelerators that rely on superconducting technology — Tevatron, HERA, CEBAF, RHIC, SSC, LEP, KEK and others — provide exciting experimental opportunities for high energy and nuclear physicists, that could not be obtained or afforded using conventional accelerator technology. The primary applications are in the

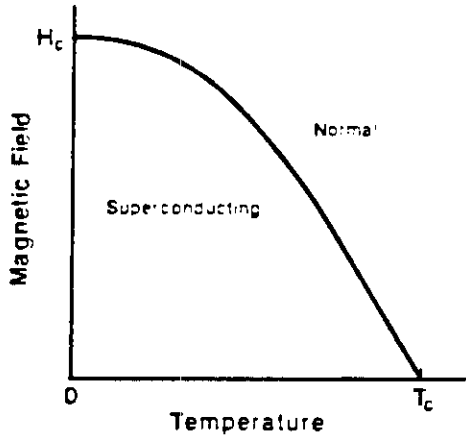


Fig. 3. Generic phase diagram for a superconductor

layer at the surface of the superconductor to produce a magnetic field inside the superconductor which exactly counterbalances the external or applied field there. The applied magnetic field penetrates the superconductor, but its magnitude drops exponentially over the London penetration depth ( $\lambda$ ), which is typically on the order of  $5 \times 10^{-2} \mu\text{m}$ . The surface currents induced in a material as it becomes superconducting persist indefinitely without degradation. To avoid such persistent currents, it is important to ensure that devices pass through the superconducting transition in the absence of a magnetic field.

Another length scale, the coherence length ( $\xi$ ), is also important to a phenomenological understanding of superconductors. The coherence length is a measure of the distance over which the superconducting properties can vary significantly, and it is related to the mean free path of normal electrons. Based on the relationship between  $\lambda$  and  $\xi$ , superconductors display distinct behavior (Figure 4).

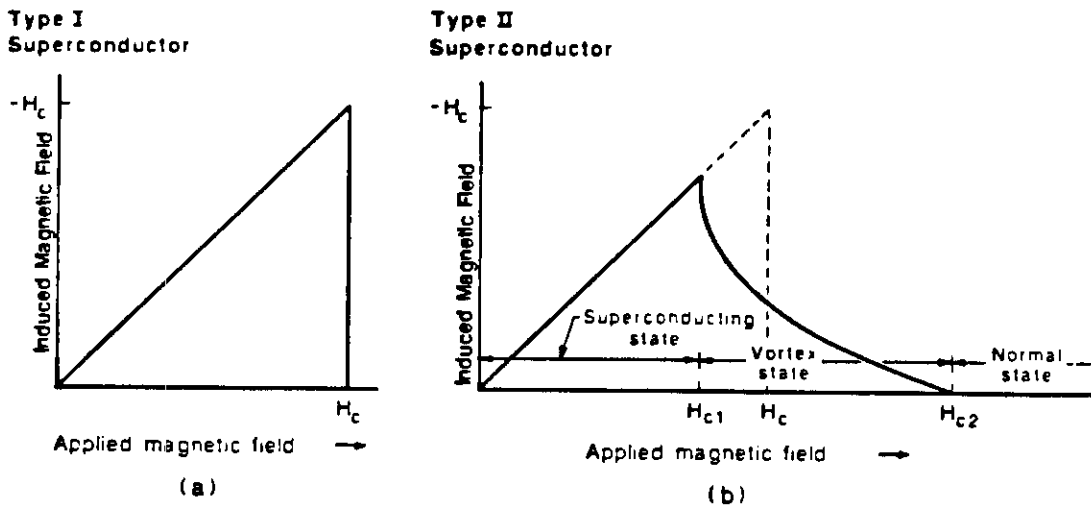


Fig. 4. Magnetic behavior of (a) Type I superconductor and (b) Type II superconductor.

Type I or "soft" superconductors have  $\xi \gg \lambda$ . For these materials, such as lead and mercury and most other elemental superconductors, the Meissner effect is close to perfect. They tend to have a low critical temperature ( $T_c$ ) and a low critical magnetic field. The induced magnetic field increases to exactly compensate the applied magnetic field until  $H_c$  is exceeded (Figure 4a), and the material becomes normal.

Type II or "hard" superconductors have  $\xi \ll \lambda$ . In these superconductors, the B field is excluded completely only up to a field,  $H_{c1} < H_c$ , and it penetrates completely above  $H_{c2} \gg H_c$  (Figure 4b). In magnetic fields between  $H_{c1}$  and  $H_{c2}$ , the magnetic field is only partially excluded, and the material exists in a so-called vortex state. Magnetic flux lines or fluxoids pass through the superconductor, and in the microscopic core of each fluxoid, the material is in a normal state. The supercurrent,  $J_s$ , flows around the perimeter of each fluxoid, thereby supporting the flux lines.

The major advantage of Type II superconductors is that superconducting electrical properties prevail up to  $H_{c2}$ . Type II superconductors are usually compounds or alloys. Examples include NbTi, Nb<sub>3</sub>Sn, and V<sub>3</sub>Ga. Typically they have a high critical temperature, and  $H_{c2}$  can be high enough to be useful in high-field magnets (Table 1). Ginzburg and Landau<sup>4</sup> developed a theory based on a two-fluid model (normal electrons and super electrons) which is useful for understanding Type II superconductors at temperatures near  $T_c$ .

Table 1  
Properties of Some Superconductors

Material	Crystal structure	$T_c$ (K)	Energy Gap ( $k_B T_c$ )	$H_{c2}(0)$ (Tesla)	$H_c(0)$ (Tesla)	Availability*
Pb	fcc	7.2	2.17	Type I	0.08	RF
Nb	bcc	9.2	1.90	.38	.19	RF
Nb <sub>3</sub> Al	A15	18.8	2.15	29.5	.65	--
Nb <sub>3</sub> Ga	A15	20.3		33.5		Exp
Nb <sub>3</sub> Ge	A15	23.6	2.1	37.0		Exp
NbN	B1	16.1	1.74	15.3	.22	Exp
Nb <sub>3</sub> Sn	A15	18.3	2.25	22.5	.53	Wire
NbTi	bcc	9.8	1.9	14.8	.24	Wire
V <sub>3</sub> Ga	A15	15.0		35.0	.74	Wire
V <sub>3</sub> Si	A15	17.1	1.78	15.6	.60	Exp
MoRe <sub>57</sub>		14	1.8	2.8	.16	Exp
PbMo <sub>6</sub> S <sub>8</sub>		14		55		--

\*RF = rf structures; Wire = wire or cable; Exp = experimental use for wire or rf  
From H. Piel (Wuppertal)

In 1956 Bardeen, Cooper, and Schrieffer<sup>5</sup> developed a successful microscopic, quantum mechanical theory of superconductivity, which underlies present understanding. According to this theory, the superconducting state is a zero-momentum state. A lattice-mediated interaction binds the electrons into "Cooper pairs", which have zero momentum and carry the supercurrent.

Several superconductors have demonstrated or potential application in accelerator magnets and rf structures. Properties of some promising ones are tabulated in Table 1, and materials with high  $T_c$  and  $H_{c2}$  are particularly attractive. To be useful, however, these materials must have satisfactory mechanical properties, and be able to be produced in quantity with the required purity in wire and/or sheet.

## ACCELERATOR MAGNETS

Accelerator magnets are designed to produce the desired magnetic field and field quality within the beam aperture. There are three basic approaches. In an iron-dominated magnet, the shape of the iron controls the shape of the field, and the field is limited to about 2 Tesla by iron saturation. In a conductor-dominated magnet the placement of the conductor controls the shape of the field, and high currents made possible by superconducting coils make high fields achievable. A hybrid design uses superconducting coils to push the field strength beyond iron saturation; hence these magnets are called "superferric". The shape of the iron and conductor placement together determine the shape of the field. Superconducting accelerator magnets are reviewed in detail by Palmer and Tollestrup<sup>6</sup>.

Superconducting accelerator magnets can provide higher magnetic fields at significantly lower power usage than can be achieved with conventional accelerator magnets. Table 2 shows the experience with FNAL Main Ring and Tevatron magnets (Figure 5). With the 4.4-Tesla superconducting Tevatron<sup>7</sup> magnets, the beam energy is doubled

Table 2  
Magnet Power Consumption at FNAL

	FNAL Main Ring (1982)	Tevatron (1984)	Ratio <u>Tevatron</u> Main Ring
Beam energy (GeV)	400	800	2.0
Electric power per flat-top time (KW hr/sec)	175	38	0.2

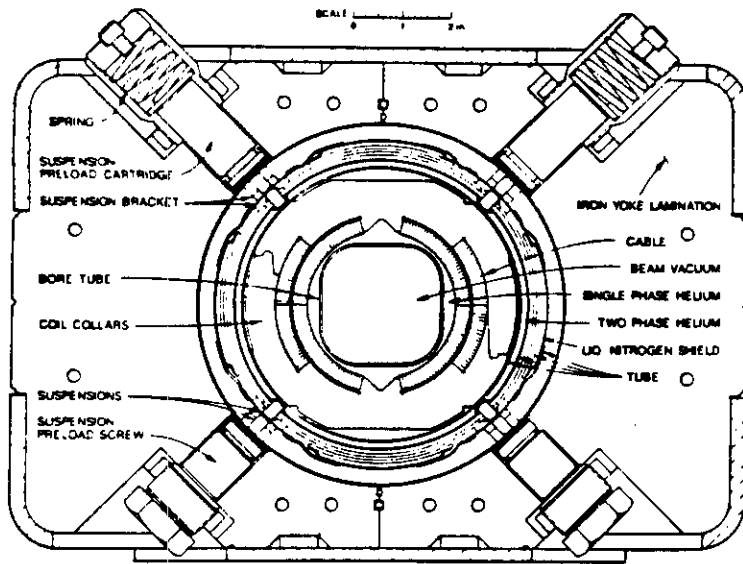


Fig. 5. Cross section of the 4.4-Tesla Tevatron<sup>7</sup> dipole magnet.

The magnetic field in a conductor-dominated magnet is determined by the current in the coils and the coil geometry. To achieve a high field requires a high current density,  $J_c$ , in the coils, and coil placement close to the aperture. Note that the achievable magnetic field is limited by the magnetic field tolerance of the superconductor. Operation at low temperatures and use of materials with high  $H_{c2}$

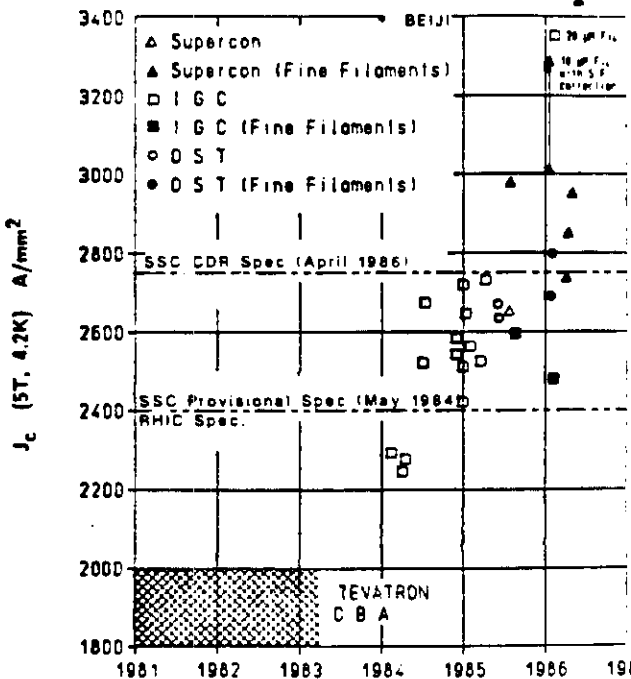


Fig. 6. Recent improvements in  $J_c$  of commercial NbTi magnet wire.

and the electric power it takes to produce each second of beam time useful for experiments (flat-top time) is only one-fifth that of the conventional Main Ring magnets.

- There are several important aspects to the design of superconducting accelerator magnets:
- o Field strength
  - o Field quality
  - o Quench protection
  - o Cost

bring clear advantages.<sup>c2</sup> Currently a NbTi alloy (46% Nb, 54% Ti) is the center of development, because it has superior mechanical properties, and can be formed into wire and cable. A major R&D challenge is to develop processes for preparing wire and cable made of Nb<sub>3</sub>Sn, which is brittle, and other materials with high  $H_{c2}$  and  $T_c$ .

With the focus on NbTi, recent R&D in support of magnet development for the Superconducting Super Collider (SSC) has resulted in a 70% improvement in  $J_c$  since 1983 in industrially produced wire (Figure 6).

This improvement is due to increased homogeneity in the NbTi alloy, an improved heat treatment and processing schedule, and the use of diffusion barriers to allow highly uniform, fine filaments to result from the drawing process<sup>8</sup>. Multifilament superconducting magnet wire is drawn from large billets containing many rods of NbTi imbedded in a copper matrix. In succeeding steps the billet is drawn to smaller diameters until each NbTi rod becomes a wire filament 5 to 20  $\mu\text{m}$  in diameter. In this process, the NbTi tends to react with the copper matrix, forming a titanium-copper intermetallic phase that disfigures the filaments (Figure 7). The intermetallic phase interferes with the flow of supercurrent, thereby limiting  $J$ . The use of a niobium jacket around each NbTi rod provides a diffusion barrier that prevents the intermetallic phase from forming (Figure 8). The resulting filaments are fine, smooth, and uniform (Figure 9).



Fig. 7. SEM micrograph of NbTi filaments with large nodules of intermetallic. Source: Lawrence Berkeley Laboratory

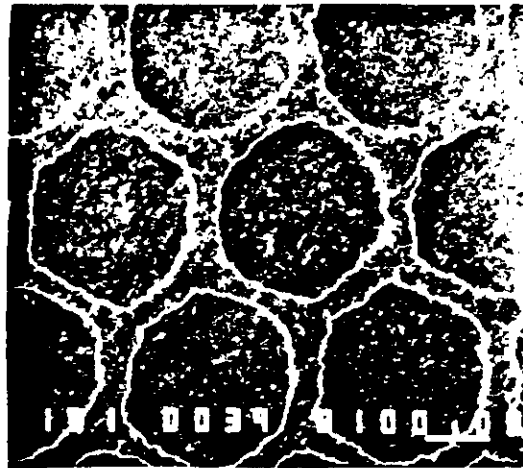


Fig. 8. Niobium-clad NbTi filaments in a copper matrix. Source: Lawrence Berkeley Laboratory



Fig. 9. SEM micrograph of niobium-clad NbTi filaments. Source: Lawrence Berkeley Laboratory

The field quality in a superconducting accelerator magnet is set by the tolerances on conductor placement and mechanical stability, and the compensation or suppression of higher order field multipoles, especially sextupole components due to persistent currents. Superconducting magnets are designed carefully to achieve and maintain the very precise conductor placement, despite the strong forces acting on the coils when the current is on.

In addition, magnets must be designed to be protected against damage during a quench. In a quench, a region of superconductor goes normal and can no longer carry the high  $J_c$ . Two alternative approaches are viable in principle: design the cable so that it can carry the current without damage through the copper matrix; or design the magnet so that the quench propagates sufficiently rapidly to avoid damage. The first alternative is not practical for accelerator magnets, because it requires a high ratio of copper to superconductor (~20:1). Therefore it can handle only a limited average current density and achieve a limited field in the beam aperture. The second alternative uses a low ratio of copper to superconductor (1.3:1 to 1.8:1) and a coil design that allows the quench to propagate longitudinally and radially. This approach ensures that a large volume of the magnet goes normal, thereby averting severe local heating and damage. Quench propagation velocities of the order of 20m/sec are required.

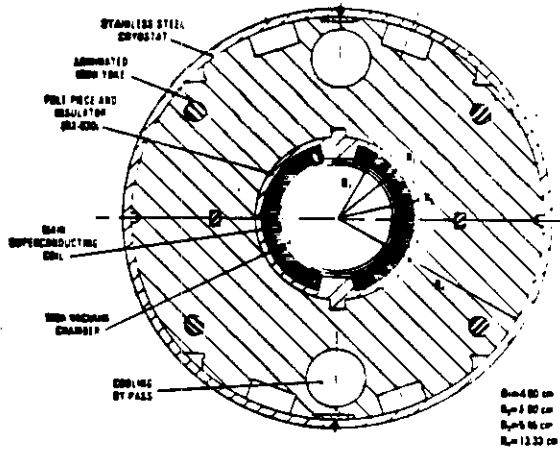
Cost issues are dominated by material requirements and assembly considerations. Since over two-thirds of a magnet's cost is in material, it is cost effective to design the magnet with the smallest aperture that is sufficient for the beam. The superconducting cable represents about 30% of the magnet's cost, so economical cable fabrication and high  $J_c$ , which reduces the amount of superconductor required, are desirable. Table 3 compares the actual cost of Tevatron dipoles with the estimated production cost of the 6.6-T SSC dipoles. Real progress has been made in this area.

**Table 3**  
**Costs of Superconducting**  
**Accelerator Dipole Magnets**

	Superconductor Cable	All Other Material	Labor	Unit Cost (1986 \$)
Tevatron	26%	40%	34%	65K
(4.4 T, 6.4m long, $J_c = 1800 \text{ A/mm}^2$ )	28%	41%	31%	62K*
SSC Conceptual Design	27%	48%	25%	106K
(6.6 T, 17m long, $J_c = 2750 \text{ A/mm}^2$ )	30%	53%	17%	97K*

\*Excluding design and inspection.





Single-layer NbTi Cos $\theta$ coil	
Cu: Superconductor	1.8:1
Superconductor $J_c$ spec.	2400 A/mm <sup>2</sup> at 5T
Length	9.7m
Temperature	4.5K
Quench Field	4.65 T

Fig. 10. Cross section of the 3.44-Tesla dipole for RHIC.

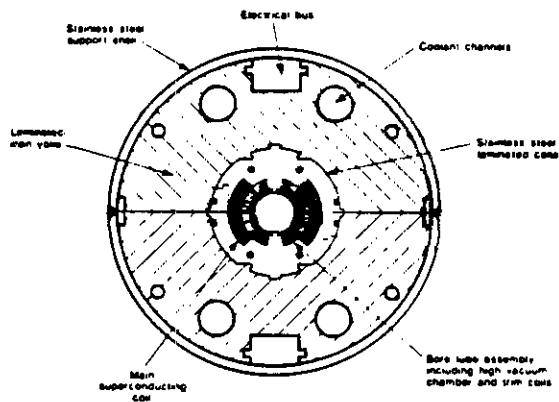


Fig. 11. Cross section of the 6.6-Tesla SSC dipole.

Two recent dipole designs bear mention.

The magnet designed at Brookhaven National Laboratory (BNL) for their proposed Relativistic Heavy Ion Collider (RHIC) has a single-layer NbTi cos $\theta$  coil (Figure 10)<sup>9</sup>. With a single layer of superconductor, this magnet is quite cost effective. It is designed to operate at 3.44 Tesla at 4.5K, well below its quench field of 4.65 Tesla.

The SSC Central Design Group<sup>10</sup> has developed a 6.6 Tesla dipole with two layers of superconducting coil (Figure 11). The aperture radius for this magnet is 2 cm, half that of the RHIC dipole, and its operating temperature is 4.35K. A stainless steel collar holds the coils firmly in position. Economical production was a major factor in the development of this design, as the SSC will require nearly 7700 units.

To achieve higher fields with NbTi superconductors, operation at 2K or below is required, and designs have three or more layers of coils. To date, both Japan (KEK) and the U.S. (LBL) have developed and tested short high-field accelerator dipoles that have achieved 9.4 Tesla and 9.3 Tesla respectively. In the future, R&D is likely to focus on increasing  $J_c$  and on superconductors, such as Nb<sub>3</sub>Sn, with high  $T_c$  and  $H_{c2}$ , to allow higher fields to be reached.

Prototype Nb<sub>3</sub>Sn magnets have been made and tested already. Work will continue on cabling and assembly procedures to reduce magnet cost and improve reproducibility and reliability of magnets fabricated in quantity by industry.

## RF ACCELERATING STRUCTURES

Radio frequency accelerating structures produce the electric field that accelerates the particle beam. Design goals for accelerating structures include achieving the desired accelerating field, with the desired frequency and frequency stability. Multipacting, field emission, and other processes that limit or degrade the field are to be avoided or minimized. Superconducting accelerating structures offer the advantages of very low rf losses. Thus, they are energy efficient, and attractive or essential for very high energy  $e^+e^-$  storage rings and colliders, TeV-scale linear  $e^+e^-$  colliders, and free electron lasers. The low losses also make CW operation feasible, both for electron linacs and heavy-ion linacs. Accelerating structures are not exposed to high magnetic fields; therefore Type I superconductors, as well as Type II superconductors can be used. The most common material employed today is niobium. R&D on rf superconductivity is underway at many laboratories and universities around the world<sup>11</sup>, and much progress has been made within the past few years<sup>12</sup>.

For low- $\beta$  accelerators, such as heavy-ion linacs, the resonator normally operates at around 100 MHz. The geometry and size of the resonator determine the resonant frequency. Typically field emission and mechanical stability limit the achievable gradient. Several heavy-ion linacs are currently in operation or under construction (Table 4)<sup>13</sup>. Most serve as boosters to increase the beam energy available at tandems.

Table 4  
HEAVY ION SUPERCONDUCTING  
BOOSTER LINACS (low  $\beta$ )<sup>13</sup>

System	Superconductor	Resonator type	$f_{rf}$ (MHz)	Active length (m)	Number of Resonators
<b>Operating</b>					
ANL Atlas	Nb	split ring	97	13.3	42
SUNY Stony Brook	Pb	split ring	150	7.5	40
Weizmann Institute	Pb	quarter wave	162	0.7	4
<b>Under construction</b>					
Saclay	Nb	helix	135	12.5	50
Florida State	Nb	split ring	97	4.5	13
Oxford	Pb	split ring	150	2.1	9
U. of Washington	Pb	quarter wave	150	8.8	36
<b>Under development</b>					
Canberra	Pb	quarter wave	150	0.8	4
Kansas State	Nb	split ring	97	3.5	16

Both niobium and lead-on-copper resonators have been used successfully. Niobium resonators have lower rf losses than lead; they therefore are more economical to operate. Lead-on-copper structures are extremely inexpensive to manufacture, however. Resonators made of both materials achieve gradients of about 3 MV/m in operation. Three ATLAS resonators (Argonne) are shown in Figure 12. Note that these three resonators, from the beginning, middle, and end of ATLAS are different. In a low- $\beta$  linac the resonators must be matched to the  $\beta$  of the particles, which increases along the length of the machine. In addition, the resonators are designed to have a broad velocity acceptance.

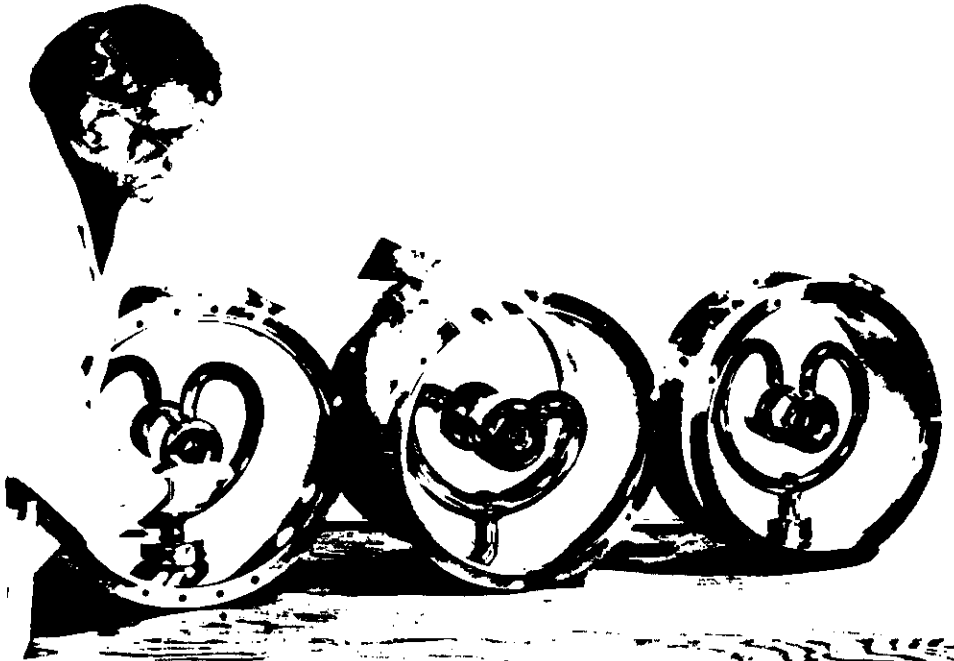


Fig. 12. Resonators for the heavy-ion linac ATLAS. Source: Argonne National Laboratory.

For  $\beta=1$  structures, resonant cavities are used<sup>11</sup> (Figure 13). The cavity size and shape determine the resonant frequency. Surface defects, multipacting, and field emission must be controlled to achieve high gradients. Higher order modes must be suppressed to achieve beam stability.

Major R&D efforts have been underway for several years at Stanford, Karlsruhe, Cornell, CERN, DESY, Wuppertal, Orsay, and KEK to develop  $\beta=1$  superconducting rf structures<sup>11</sup>. Until recently, achieved gradients were limited to about 3 MV/m. Now gradients in excess of 5 MV/m are achieved routinely, at laboratories and by industry (Table 5). The theoretical gradient limit is  $\sim 50$  MV/m for Nb and  $\sim 80$  MV/m for Nb<sub>3</sub>Sn. Recent progress has been very rewarding, and there are firm plans now to employ these structures in several planned accelerators and major upgrades (Table 6).

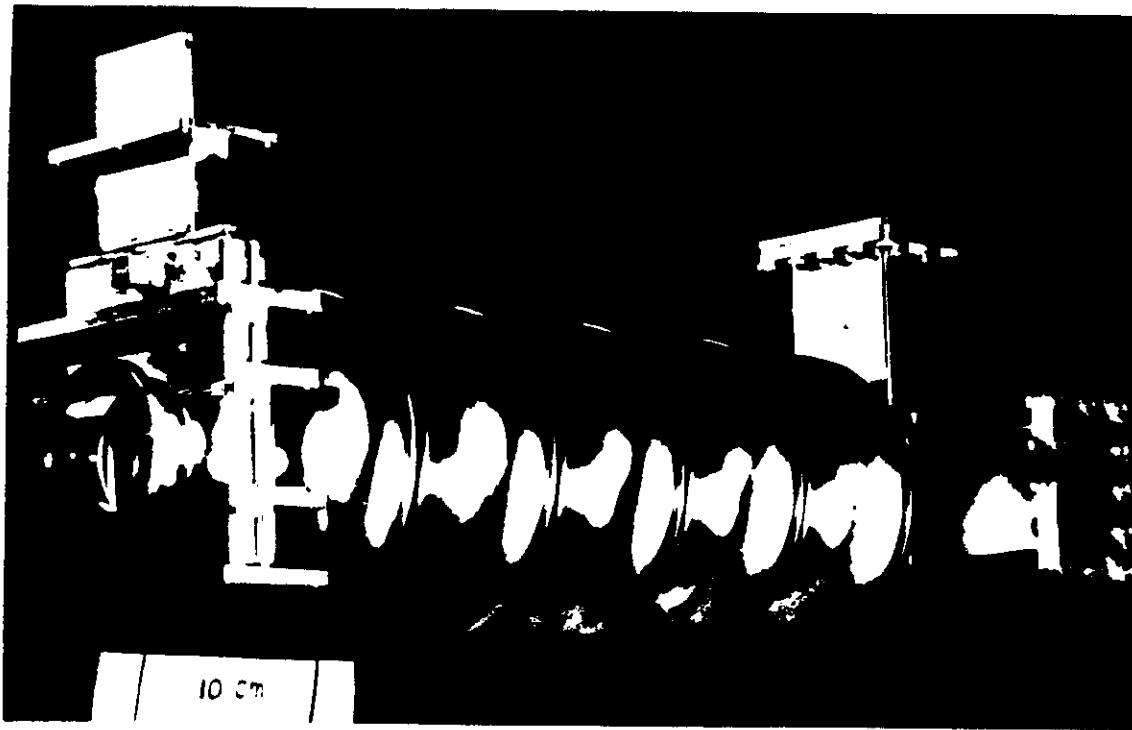


Fig. 13. Five-cell, 1500-MHz cavity designed by Cornell and adopted by CEBAF.

Table 5

PERFORMANCE OF  $\beta=1$  SUPERCONDUCTING RF CAVITIES  
(From H. Piel, Wuppertal)

Laboratory	CERN			KEK	DESY	Cornell	CEBAF**	Darmstadt/Wuppertal	
Accelerator	LEP II			TRISTAN	HERA	CESR	CEBAF	130 MeV	Recyclotron
Material	Nb	Nb	Nb/Cu	Nb	Nb	Nb	Nb	Nb	Nb <sub>3</sub> Sn
Frequency in MHz	350	500	500	500	1000	1500	1500	3000	3000
Operating Temperature	4.2K	4.2K	4.2K	4.2K	4.2K	1.8K	2.0K	1.8K	4.2K
<u>Best Single-Cell Results</u>									
$E_A$ (MV/m)	10.8	13.0*	10.8	7.6*	5.5	22.8*	-	23.1*	7.2
Q At $E_A$ ( $\times 10^9$ )	1.8	0.7	0.4	0.6	0.5	2.5	-	1.2	1.1
<u>Best Multicell Results</u>									
No. of Cells	4	5	-	3	9	5	5	5/20	5
$E_A$ (MV/m)	7.5*	5.8	-	5.8	5.5	15.3*	7.9*	12.3/7.4	4
Q At $E_A$ ( $\times 10^9$ )	2.2	0.7	-	0.6	0.5	2.2	6.0	3.5/1.2	4.5

\* Cavities Fabricated From High Thermal Conductivity Niobium  
\*\* Cornell Cavity design

**Table 6**  
**PLANNED APPLICATION OF**  
 **$\beta=1$  SUPERCONDUCTING CAVITIES**

<u>Laboratory</u>	<u>Accelerator</u>	<u>Frequency</u> <u>MHz</u>	<u>Active</u> <u>Length (m)</u>
CERN	LEP I, 50 GeV	350	20
CERN	LEP II, 100 GeV	350	650
CEBAF	4 GeV Linac	1500	200
DESY	HERA e, 30 GeV	500	20
KEK	TRISTAN, 33-35 GeV	508	60
KEK	TRISTAN, 40 GeV	508	180-216
Wuppertal/ Darmstadt	130 MeV Linac	3000	12
HEPL/TRW	Free Electron Lasers	1300/ 500	5-6
?	TeV Linear Collider	~1000-3000	~8x10 <sup>4</sup>

From H.Padamsee

The major design issues for rf cavities are:

- o Frequency selection and stability
- o Cavity shape
- o Superconductor selection, processing, and cleanliness
- o Cost

Prototype  $\beta=1$  rf cavities have been built to operate at several frequencies between 350 MHz and 8000 MHz. For low frequencies, the cavities are big, awkward to handle, and have a high probability of having a serious defect somewhere on the cavity surface. However, intrinsic RF losses (BCS losses) increase with frequency squared, and deflecting impedances that limit beam current increase as frequency cubed. Thus, the optimum frequency for a specific accelerator will depend on that accelerator's specifications.

Cavity shape is an important factor for both cost and performance. Within the past few years, several improvements in this area have been developed. Spherical or elliptical cell shape has been shown to reduce multipacting. Couplers for fundamental power and for higher order mode (HOM) suppression attach to the beam pipe to minimize field enhancement and multipacting. The number of individual resonant rf cells (half wavelength) in a cavity is limited to control HOMs. Very early rf cavity development at Stanford's High Energy Physics

Laboratory (HEPL) resulted in cavities with 55 cells, and serious HOM problems. Current designs (Table 5) call for five cells or fewer. Cavity design and HOM suppression are aided now by the availability of computer codes, such as URMEL<sup>14</sup>.

The most common superconductor currently in use for  $\beta=1$  accelerating structures is niobium. Since only a very thin surface layer on the inside of the cavity is active in the formation of the accelerating field, the quality and cleanliness of that surface layer is of the utmost importance to cavity performance. In addition, the surface layer must be kept below the superconducting transition temperature: cooling must be adequate to remove the heat generated by rf dissipation in dust and defects.

Recent developments in niobium processing and cavity fabrication have resulted in real progress in these areas. Niobium suppliers have developed the capability to produce niobium sheet with high thermal conductivity (RRR). High thermal conductivity helps to stabilize the cavity against being driven normal by resistive heating at a defect. Yttrification has been developed as a process to increase the thermal conductivity<sup>15</sup>. The availability of clean rooms and clean manufacturing protocols avoids the introduction of dust or dirt on the active surface. Refined electron beam welding methods help achieve weld smoothness.

Another recent development is thermometric mapping to locate hot spots caused by defects or dirt on the superconducting surface. A cavity can be tested and the factor limiting its gradient can be located and repaired. With the assistance of Cornell University's SRF Group, CEBAF has been working with four vendors to fabricate prototype cavities for CEBAF's 4-GeV CW electron linac. Each delivered cavity is tested to ensure that it meets or exceeds CEBAF's specifications for gradient (5 MV/m) and  $Q$  ( $3 \times 10^9$ ). To date four cavities have been completed by three vendors. All four cavities exceed the specifications (Figure 14). Cavity Number 3 has been tested twice, and undergone "repair" to remove the defect that limited the gradient to 6.8 MV/m on the first test.

Although gradients of 5 to 10 MV/m are achieved by industry today in prototype cavities, the real attraction of rf structures is their potential to achieve gradients in excess of 20 MV/m with very low rf losses (high  $Q$ ) and high beam-current capacity. Single-cell cavities fabricated at Cornell and Wuppertal have achieved such high gradients (Table 5). According to Sundelin<sup>16</sup>, TeV-scale linear colliders become economically feasible at a gradient of about 25 MV/m and a quality factor ( $Q$ ) of  $5 \times 10^{10}$ .

Experimentation is underway with Nb<sub>3</sub>Sn, niobium on copper, and other superconductors as cavity materials. Nb<sub>3</sub>Sn offers the potential for lower rf losses and operation at higher temperatures. Niobium on copper would have a very high thermal conductivity, hence excellent stabilization of submicroscopic defects and dust.

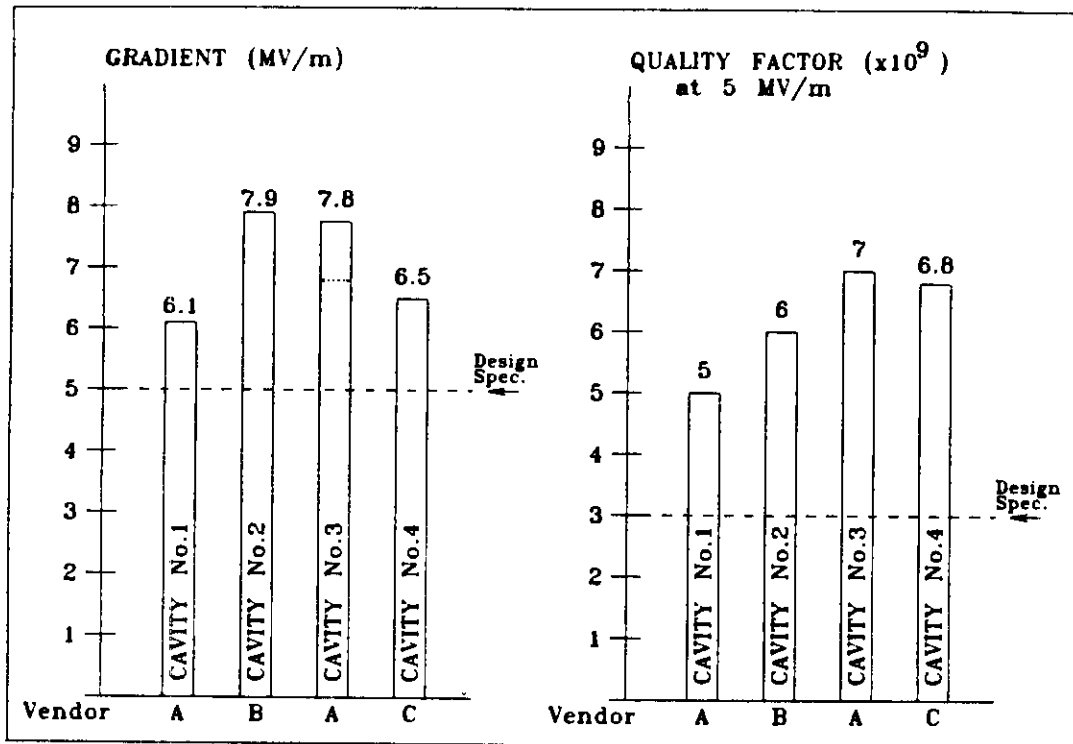


Fig. 14. Preliminary results from CEBAF's cavity prototyping program

## CONCLUSIONS

Both in accelerator magnet development and in rf structure development, superconducting technology has reached a sufficient level of performance and reliability to become practical and cost effective. In both areas, the technology is young, and foreseeable improvements promise far greater capabilities in the future, that will serve as the basis for new accelerators and upgrades required by high energy and nuclear physicists to advance the frontiers of knowledge.

## REFERENCES

1. H. K. Onnes, Commun. Phys. Lab. Univ. Leiden Suppl. 34b, 55 (1913).
2. W. Meissner and R. Ochsenfeld, Naturwissenschaften 21, 787 (1933).
3. F. London and H. London, Proc. R. Soc. London, Ser A, 149 (1935).
4. V. L. Ginzburg and L. D. Landau, J. Exp. Theor. Phys. (USSR) 20, 1064 (1950).
5. J. Bardeen, L. N. Cooper, and J. R. Schrieffer, Phys. Rev. 108, 1175 (1957).

6. R. Palmer and A. V. Tollestrup, *Ann. Rev. Nucl. Part. Sci.* 34, 247 (1984).
7. H. T. Edwards, *Ann. Rev. Nucl. Part. Sci.* 35, 605 (1985).
8. R. Scanlan, Lawrence Berkeley Laboratory, personal communication (May 1986); see also D. Larbalestier, *Proc. 9th Intl. Conf. Magnet Tech, SIN*, 453 (1985).
9. Proposal for a Relativistic Heavy Ion Collider, BNL 51932 (1986).
10. Superconducting Super Collider Conceptual Design, SSC-SR-2020 (1986).
11. H. Lengeler, ed., *Proc. 2nd Workshop on RF Superconductivity, CERN* (1984).
12. H. Piel, in *Proc. 1985 Part. Accel. Conf., IEEE Trans. Nucl. Sci. NS32* (1985).
13. L. M. Bollinger, *Nucl. Instr. and Meth.* A244, 246 (1986).
14. T. Weiland, *DESY Rept. 82-015* (1982).
15. H. Padamsee, in *Proc. 1985 Part. Accel. Conf., IEEE Trans. Nucl. Sci. NS32* (1985).
16. R. Sundelin, Cornell University, CLNS 85/709 (1985).

Superconducting accelerator technology is under development at many laboratories. This work was supported by the Department of Energy under contract DE-ACO-84ER4015, and by the Commonwealth of Virginia.